Journal of Controlled Release 375 (2024) 614–626

Contents lists available at ScienceDirect

Journal of Controlled Release

journal homepage: www.elsevier.com/locate/jconrel

Microfluidic formulation, cryoprotection and long-term stability of paclitaxel-loaded π electron-stabilized polymeric micelles

Rahaf Mihyar [a], Armin Azadkhah Shalmani [a], Viktor Wildt [a], Maryam Sheybanifard [a], Alec Wang [a], Jan-Niklas May [a], Saba Shahzad [b], Eva Miriam Buhl [c], Stephan Rütten [c], Diana Behrens [d], Wolfgang Walther [d], Mattia Tiboni [e], Luca Casettari [e], Johannes F. Buyel [f], Cristianne J.F. Rijcken [g], Wim E. Hennink [h], Saskia von Stillfried [i], Fabian Kiessling [a], Yang Shi [a], Josbert M. Metselaar [a], Twan Lammers [a,*], Quim Peña [a,*]

[a] Institute for Experimental Molecular Imaging, RWTH Aachen University Hospital, Forckenbeckstrasse 55, 52074 Aachen, Germany
[b] Ernst Ruska-Centre for Microscopy and Spectroscopy with Electrons (ER - C -3): Structural Biology, Forschungszentrum Jülich, Wilhelm-Johnen-Straße, 52428 Jülich, Germany
[c] Electron Microscopy Facility, Institute of Pathology, RWTH Aachen University Hospital, Pauwelsstrasse 30, 52074 Aachen, Germany
[d] Experimental Pharmacology and Oncology GmbH, Robert-Roessle-Str. 10, 13125 Berlin, Germany
[e] University of Urbino Carlo Bo, Department of Biomolecular Sciences, Via Ca' le Suore 2/4, 61029, Urbino (PU), Italy
[f] Institute of Bioprocess Science and Engineering (IBSE), University of Natural Resources and Life Sciences (BOKU), Department of Biotechnology, Muthgasse 18, 1190 Vienna, Austria
[g] Cristal Therapeutics, Oxfordlaan 55, 6229 EV Maastricht, the Netherlands
[h] Department of Pharmaceutics, Utrecht Institute for Pharmaceutical Sciences, Faculty of Science, Utrecht University, 3508 TB Utrecht, the Netherlands
[i] Institute of Pathology, RWTH Aachen University Hospital, Pauwelsstrasse 30, 52074 Aachen, Germany

ARTICLE INFO

Keywords:
Nanomedicine
Polymeric micelles
Cryoprotectants
Microfluidics
Flow manufacturing

ABSTRACT

Controlled manufacturing and long-term stability are key challenges in the development and translation of nanomedicines. This is exemplified by the mRNA-nanoparticle vaccines against COVID-19, which require (ultra-) cold temperatures for storage and shipment. Various cryogenic protocols have been explored to prolong nanomedicine shelf-life. However, freezing typically induces high mechanical stress on nanoparticles, resulting in aggregation or destabilization, thereby limiting their performance and application. Hence, evaluating the impact of freezing and storing on nanoparticle properties already early-on during preclinical development is crucial. In the present study, we used prototypic π electron-stabilized polymeric micelles based on mPEG-*b*-p(HPMAm-Bz) block copolymers to macro- and microscopically study the effect of different cryoprotective excipients on nanoformulation properties like size and size distribution, as well as on freezing-induced aggregation phenomena via in-situ freezing microscopy. We show that sucrose, unlike trehalose, efficiently cryoprotected paclitaxel-loaded micelles, and we exemplify the impact of formulation composition for efficient cryoprotection. We finally establish microfluidic mixing to formulate paclitaxel-loaded micelles with sucrose as a cryoprotective excipient in a single production step and demonstrate their stability for 6 months at −20 °C. The pharmaceutical properties and preclinical performance (in terms of tolerability and tumor growth inhibition in a patient-derived triple-negative breast cancer xenograft mouse model) of paclitaxel-loaded micelles were successfully cryopreserved. Together, our efforts promote future pharmaceutical development and translation of π electron-stabilized polymeric micelles, and they illustrate the importance of considering manufacturing and storage stability issues early-on during nanomedicine development.

* Corresponding authors.
E-mail addresses: tlammers@ukaachen.de (T. Lammers), jpena@ukaachen.de (Q. Peña).

https://doi.org/10.1016/j.jconrel.2024.08.041
Received 15 April 2024; Received in revised form 20 July 2024; Accepted 25 August 2024
Available online 23 September 2024

1. Introduction

Manufacturing is a key challenge in the clinical translation of nanomedicines [1,2]. Measures to control batch-to-batch reproducibility and ensure long-term stability of nanoformulations are crucial in pharmaceutical development, as observed during the recent surge of mRNA-loaded lipid nanoparticles (LNPs). The COVID-19 pandemic and the development of the mRNA LNP-based vaccines underscored the importance of robust large-scale nanomedicine production, including control and preservation of critical quality attributes (CQA) during manufacturing, distribution, handling, and storage [3–5].

Nanoparticle-based drug delivery systems prepared in lab settings typically use bench-scale (batch) preparation methods that can be challenging to control at industrial-scale [1]. Several formulation properties, such as nanoparticle size, polydispersity, and drug retention capability can affect the eventual (in vivo) performance of nanomedicines. Continuous-flow manufacturing technologies have been gaining attention for controlling the preparation and CQA of different types of nanoformulations, including lipid- [6] and polymer-based nanoparticles [7,8]. In this regard, methods like microfluidic mixing facilitate large-scale production and contribute to streamlining manufacturing procedures, making the overall process more robust, efficient, and cost-effective.

Stability during shipment, handling and long-term storage is another key aspect to consider during industrial production, preserving performance and ensuring commercial feasibility and applicability of pharmaceutical products. To increase the shelf-life of nanomedicine drug products, several freezing strategies have been explored, such as storage at cryogenic temperatures [9] or freeze-drying procedures [10]. Both methods are established in pharmaceutical manufacturing and have been used to increase the shelf-life of different (nano)pharmaceuticals. Storage at cryogenic temperatures is applicable to a broad range of nanoparticle classes and drug payloads, including the mRNA-LNP vaccines. However, the freezing step presents a key challenge due to the high mechanical stress induced on the nanoparticles during ice crystal formation, which can result in aggregation, destabilization, and drug leakage [11], together impairing the usability of the final product [12].

To preserve the properties of (nano)formulations during freezing, cryoprotectants (CPs) such as saccharides, polymers, and surfactants are used to prevent formation of ice crystals and attenuate aggregation. Disaccharides, particularly sucrose and trehalose, are amongst the most frequently used cryoprotective excipients in pharmaceutical formulations [12,13]. While CPs have already been included in several nanomedicine drug products such as the mRNA LNP-based COVID-19 vaccines Comirnaty and Spikevax, cryopreservation protocols are not universally applicable, and the right choice of CP and its optimal concentration are highly dependent on nanoparticle type and specific composition [14]. To date, several studies have reported the impact of CPs and freezing (or freeze-drying) strategies on nanomedicine formulations, quite prominently on lipid- [10,15,16] and protein-based [13,17]. Others, like polyplexes [18] and inorganic nanoparticles [19] have been also investigated in this regard. However, considerably less attention has been given to polymeric systems like polymeric micelles.

Polymeric micelles are amongst the most extensively studied nanoscale drug delivery systems. They are based on amphiphilic block copolymers that self-assemble in aqueous media into micellar structures constituted of a hydrophilic shell and a hydrophobic core, in which poorly water-soluble drugs can be encapsulated. Many preclinical and several clinical studies have shown the potential of polymeric micelle-based formulations in cancer therapy [20–22], exemplified by the clinically approved paclitaxel micellar formulation Genexol-PM. Over the last decades, various systems based on *N*-(2-hydroxypropyl) methacrylamide (HPMA) polymers have been investigated for anticancer drug delivery, owing to their biocompatibility and multifunctionality [23,24]. In particular, micelles stabilized via physical interactions have attracted attention because of their versatility, high drug loading capacities, and ease of formulation. A notable example is a π electron-stabilized polymeric micelle platform based on methoxy poly(ethylene glycol)-b-(*N*-(2-benzoyloxypropyl) methacrylamide (i.e., mPEG-*b*-p(HPMAm-Bz)) block copolymers [25]. This platform has shown high tunability, and can efficiently (co-)encapsulate different drugs, such as taxanes and corticosteroids, through hydrophobic and π-π interactions [26–28]. Taxane-loaded micelles have already demonstrated promising preclinical performance in different animal models, and this specific micelle platform is currently under evaluation for scale-up development and translation [8,29,30]. However, the fact that the self-assembly and drug encapsulation processes of this type of micelles are driven by physical interactions rather than by chemical bonds (as in core-crosslinked polymeric micelles [31]) can lead to lower formulation stability during storage, and thereby compromise commercialization and clinical applicability.

In this work, we set out to explore and expand the shelf-life, storage stability, and future manufacturing potential of physically stabilized polymeric micelles (Fig. 1). We used the π electron-stabilized [mPEG-*b*-p

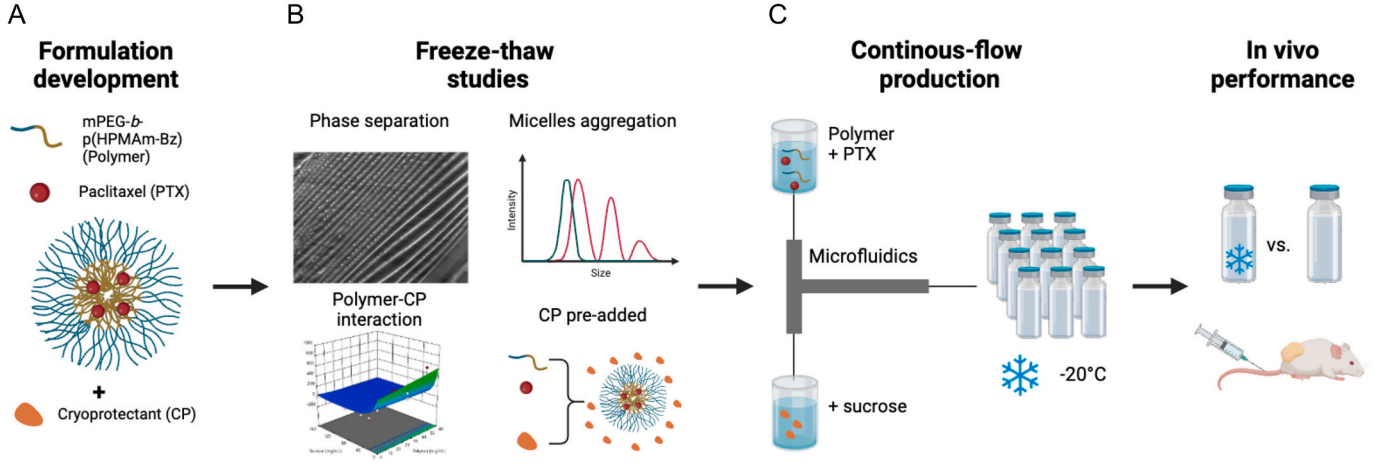

Fig. 1. Cryoprotection and long-term stability evaluation of π electron-stabilized paclitaxel-loaded polymeric micelles formulated using microfluidics. Schematic representation of the study design. **A)** Formulation of paclitaxel (PTX)-loaded [mPEG-*b*-p(HPMAm-Bz)]-based micelles using bench-scale nanoprecipitation with and without the addition of cryoprotectants (CPs: sucrose or trehalose). **B)** Assessment of the impact of freezing protocols on the properties of PTX-loaded micelles with and without CP. Several optical and electron microscopy techniques were used to visualize phase separation and possible aggregation of the micelles. **C)** Preparation of PTX-loaded micelles using 3D-printed microfluidic chips in the presence of sucrose as a cryoprotective excipient, and evaluation of long-term stability and therapeutic performance after storage at cryogenic temperatures for several months.

(HPMAm-Bz)]-based micelle platform to investigate the impact of the freezing step on formulation properties and provide a better understanding on the mechanism responsible for nanoparticle aggregation during freezing. To this end, paclitaxel (PTX)-loaded micelles with and without disaccharides-based CPs were formulated, and the impact of these CPs on key properties of the resulting formulations was assessed. Using various microscopy techniques, we visualized the ice-induced phase separation and aggregation phenomena of the micelles upon freezing in the presence of CPs. We furthermore systematically investigated the effect of several formulation parameters on the efficient cryoprotection of the micelles to determine effective CP concentrations. Moreover, we assessed the impact of formulation and process parameters on the continuous-flow microfluidic preparation of drug-loaded micelles formulated in the presence of CP. Finally, we comparatively evaluated the stability, in vivo tolerability, and therapeutic performance of PTX-loaded micelles after being stored at cryogenic temperatures (−20 °C) for several months.

2. Materials and methods

2.1. Materials

Paclitaxel (PTX) was ordered from MP Biomedicals (Germany). Sucrose was purchased from AppliChem (Germany). Trehalose was acquired from Roth Pharma (Germany). Cyanine 7-amine (Cy7) dye was ordered from Lumiprobe (Germany). Fresh Milli-Q water was available in-house. All used organic solvents were of HPLC grade and purchased from commercial suppliers. mPEG-*b*-p(HPMAm-Bz) block copolymer (Mn ~ 22 kDa and Đ ~1.7, based on gel permeation chromatography (GPC)) was prepared following previously reported protocols [25]. Characterization data were in concordance with previous literature [28].

2.2. Micelles formulation via bench-scale (BS) nanoprecipitation method

Empty and PTX-loaded [mPEG-*b*-p(HPMAm-Bz)]-based micelles were prepared by the conventional nanoprecipitation bench-scale (BS) method [32]. Briefly, the desired polymer and PTX amount were dissolved in tetrahydrofuran (THF) and the solution was added dropwise to 1 mL of deionized MilliQ water under stirring at 1000 rpm at room temperature for 1 min. Samples were then kept at room temperature for 24 h to allow for THF evaporation. The resulting micellar dispersion was adjusted to 1 mL and filtered through 0.45 μm nylon membrane filters (Whatman, Sigma Aldrich, Germany) to remove the non-encapsulated, precipitated drug.

2.3. Micelles formulation via microfluidics (MF)

For the preparation of [mPEG-*b*-p(HPMAm-Bz)]-based micelles using microfluidics, the protocol was adapted from previously reported methods [33]. The in-house 3D-printed chips were connected to two syringes mounted on a syringe pump (Harvard Apperatus-30-3007, USA) through polyethylene tubing. The desired amounts of block copolymer and PTX were dissolved in THF and pumped against water with and without sucrose at varying total flow rates. The flow rate ratio was fixed at 1:1 (organic:aqueous phases), and the formed micelles were collected from the outlet stream. THF and non-encapsulated PTX were removed as described for the bench-scale method.

2.4. Dynamic light scattering (DLS) measurements

The hydrodynamic diameter (*Z*-average, size) and polydispersity index (PDI) of the micelle formulations were determined with DLS using a Zetasizer Nanoseries ZS90 (Malvern instruments Ltd., UK). Samples were diluted to a polymer concentration of 500 μg/mL in Milli Q water and transferred into disposable polystyrene cuvettes. The number of measurements was set to 3 with 11 runs per measurement at 25 °C while the attenuator was automatically set. Hydrodynamic diameter (size), polydispersity index (PDI), and size distribution histograms were calculated based on the autocorrelation function.

2.5. Paclitaxel (PTX) encapsulation efficiency

To assess the PTX loading content, PTX-loaded polymeric micelles were disrupted with acetonitrile (ACN) to dissolve both the polymers and the drug, filtered through 0.2 PTFE filters, and the amount of drug quantified using reversed-phase HPLC (1260 II Infinity LC system, Agilent technologies, USA). For the mobile phase, a gradient elution method was used with a ACN/water mixture ranging from 39/61 (v/v) to 65/35 (v/v) in 3 min, and containing 0.1 % trifluoroacetic acid in each solvent. The injection volume was 25 μL at a 1 mL/min flow rate using the C18 column (4.6 × 150 mm, 5 μm) as a stationary phase. UV detection was carried out at 227 nm. Standard curves were generated for PTX and were utilized for its quantification using the integrated area under the peak. PTX encapsulation efficiency (%) was calculated using Eq. (1):

$$PTX\ Encapsulation\ (\%) : \frac{Detected\ amount\ of\ drug^{*}100}{Feed\ amount\ of\ drug} \quad (1)$$

2.6. Drug release studies

The release of PTX from [mPEG-*b*-p(HPMAm-Bz)]-based micelles was evaluated in simulated physiological sink conditions, following an analog method as previously reported [34]. The release media consisted of bovine serum albumin (BSA, 45 mg/mL) dissolved in phosphate-buffered saline (PBS, pH 7.4) with the following composition: 137.9 mM sodium chloride, 1.47 mM potassium phosphate monobasic, 2.67 mM potassium chloride, 8.09 mM sodium phosphate dibasic. The PTX-loaded micelle formulations were diluted in the release media and 1 mL of this solution placed inside a dialysis device with a MWCO of 300 kDa (Float-A-lyzer G2, Repligen, USA), submerged in 250 mL of release medium, and kept under agitation at 37 °C. Sample volumes of 50 μL were withdrawn at 0, 1, 4, 6, 24, 48 and 72 h from the inner compartment and replaced with the same volume of fresh media. PTX concentration at each time point was determined using HPLC as previously described in section 2.5. At each time point, the values were also corrected for the corresponding dilution factor.

2.7. Freeze-thaw (FT) studies

To test the effect of the CPs (sucrose and trehalose) on the physicochemical properties and drug retention of the formulations, a FT cycle test was used. PTX-loaded micelles (prepared using a polymer concentration of 10 mg/mL and a drug feed amount of 1 mg/mL via the BS nanoprecipitation method described in section 2.2) were diluted by 20 % with concentrated stock solutions of each CP in water to achieve a final CP concentration of 100 mg/mL. For a single FT cycle test, samples were snap-frozen in liquid nitrogen for 30 s and then were allowed to thaw at room temperature. Size and PDI of the micelles before and after FT were determined as described in section 2.4. In order to assess the encapsulated PTX after a FT cycle, samples were centrifuged at 5000 x*g* for 10 min (Heraeus Pico 21 Microcentrifuge, ThermoFischer Scientific, Germany) to remove the precipitated drug, and the PTX content in the supernatant was quantified as described in section 2.5.

2.8. Transmission electron microscopy (TEM)

For TEM analysis, micelle formulations were diluted to a final concentration of 100 μg/mL of block copolymer in Milli-Q water. The samples were left to adsorb on glow discharged from formvar-carbon-coated nickel grids (Maxtaform, 200 mesh, Plano, Wetzlar, Germany) for 10 min. Negative staining was performed with 0.5 % uranyl acetate

(Science Services GmbH, Munich, Germany). TEM images were recorded on a Hitachi HT7800 (Hitachi, Tokyo, Japan), operating at an acceleration voltage of 100 kV.

2.9. Cryogenic-transmission electron microscopy (cryo-TEM)

Micelle morphology before and after FT, and with and without CPs, was assessed using cryogenic transmission electron microscopy (cryo-TEM). Prior to vitrifying the sample on the copper 200 mesh grid with carbon R2/1 foil (Quantifoil Micro Tools GmbH, Germany), the grid was made hydrophilic by glow discharging in a PELCO easiGlow device (Ted Pella Inc., CA, USA) for 60 s at 15 mA and 0.4 mBar. The different micelle formulations were diluted to a final concentration of 10 μg/mL. Subsequently, 0.5 nL of the sample were precision-printed onto the grid using a fully automated vitrification robot, VitroJet (CryoSol-World B. V., The Netherlands). This process occurred at room temperature and 100 % humidity, with a speed of 2 mm/s and a stand-off distance of 10 μm.

Following the pin-printing of the sample, the grid was rapidly vitrified by jetting ethane and then stored in liquid nitrogen. Imaging was performed using a Talos Arctica microscope (Thermo Fisher Scientific Inc., MA, USA) operating at 200 kV, equipped with a Gatan K3 camera and a post-column Bioquantum energy filter (Gatan Inc., CA, USA) at the Ernst Ruska Centre (ER-C), Forschungszentrum (Jülich, Germany). The final imaging was conducted at a 100,000× nominal magnification with a pixel size of 0.4 Å/pixel and a total dose of 70 e/Å using TEM Imaging & Analysis Software (TIA, Thermo Fisher Scientific).

2.10. In-situ freezing fluorescence microscopy

Freezing-induced phase separation was imaged using an Axio Imager M2 fluorescence microscope equipped with an AxioCam MRm Rev.3 camera (Carl-Zeiss, Oberkochen, Germany). This technique was modified based on a previously developed method [11]. To visualize the polymeric micelles, they were labelled with Cy7 dye, following similar protocols as previously reported [25]. Cy7-labelled micelles (40 μL) in water at a polymer concentration of 15 mg/mL, with and without 100 mg/mL of sucrose or trehalose, were deposited on a glass slide and covered with a coverslip. Freezing was induced by placing a dry ice pellet on the glass slide close to the coverslip, which was followed by removing the pellet and allowing it to thaw at room temperature. The field of view was chosen randomly on the slides and images were obtained before, during freezing, and after thawing at a magnification of 200 using the corresponding channel for Cy7 (excitation at 756 nm and emission at 799 nm).

2.11. Cryogenic-scanning electron microscopy (cryo-SEM)

For cryo-SEM analysis, a drop of micellar dispersion at a concentration of 15 mg/mL with and without the presence of 100 mg/mL of sucrose or trehalose was drop-casted on the sample holder, immediately snap-frozen with liquid nitrogen and moved to the Alto 2500 cryo-Gatan unit (Gatan GmbH, Munich, Germany). To expose a cross-sectional surface and remove the top layer of ice, fracturing was done using a cooled blade before transferring the sample into the SEM. The fractured surface was then sublimated for around 4 min at −80 °C to enhance the surface topological contrast. Images were acquired with a FE-SEM 4800 (Hitachi, Krefeld, Germany) at approximately −139 °C. The cryo-SEM was operated at an acceleration voltage between 1.0 and 2.0 kV.

2.12. Optimization of the sucrose concentration for stabilization of micelles upon freeze-thawing using design of experiments

The effect of different concentrations of polymer (4–60 mg/mL), drug (1–7.5 mg/mL) and sucrose (0–160 mg/mL) on micelle size (hydrodynamic diameter) and PDI as well as on encapsulated drug (EE) was studied in a 55-run d-optimal response surface design using a quadratic base model. The design of experiments (DoE) was set up and analyzed using Design Expert v13 (Stat-Ease). First, PTX-loaded micelles were prepared via BS nanoprecipitation method. The formulations were then diluted by 20 % (v/v) with sucrose stock solutions to achieve the final sucrose concentrations defined in the respective run of the experimental design (**Table S1**). All formulations were subjected to a single FT cycle test. Size, PDI and PTX encapsulation before and after FT were measured as described in sections 2.4 and 2.5 and the change was calculated using Eq. (2):

$$\Delta\,(size, PDI\ or\ PTX\ encapsulation) = value\ after\ FT - value\ before\ FT \quad (2)$$

Individual models were built for each of the three responses. The responses were transformed using a Log10-function if a Box-Cox analysis indicated suitability of this modification. Starting with a full quadratic model, insignificant terms (p-value >0.05) were removed unless required to maintain model hierarchy [35]. The goodness of fit of the polynomial model was assessed based on three coefficients of determination (R^2, adjusted R^2, and predicted R^2) as well as a set of residuals (e.g., normal plot of externally studentized residuals) and design analyses (e.g., leverage, Cook's distance).

2.13. Differential scanning calorimetry (DSC)

The glass transition temperature of frozen micelle dispersions (Tg') was measured using DSC. Measurements were done using DSC 8000/8500 (PerkinElmer, USA). Briefly, 20 μL of sucrose-containing PTX-loaded micelles (formulated in the presence of 80 mg/mL of sucrose in the aqueous phase using the BS method at a polymer concentration of 30 mg/mL and a PTX feed amount of 7.5 mg/mL) were transferred to a pan and were sealed with a lid. The pan was then transferred to the device and frozen to −70 °C at a cooling rate of 10 °C/min. Three cycles of heating, cooling, and heating were applied at a rate of 10 °C/min between −70 °C and 50 °C and Tg' was automatically calculated using the software.

2.14. Animal experiments

Patient-derived triple-negative breast cancer xenograft (PDX) specimens (Ma14986) were orthotopically inoculated into the right abdominal mammary gland fat pad of anesthetized 6–8 weeks old NMRI nu/nu immunodeficient female mice. Mice were randomly divided into 3 groups ($n = 5$ animals per treatment group, and $n = 4$ for the control group) and administered once weekly intravenously with either freshly prepared PTX-micelles, cryoprotected PTX-micelles (stored frozen at −20 °C and thawed at RT for 1 h prior injection) or PBS (control group). PTX-micelle formulations (30 mg/mL of polymer, drug feed amount of 7.5 mg/mL and, for the cryoprotected one, 80 mg/mL of sucrose) were administered at a PTX dose of 30 mg/kg of body weight and a volume of 8.3 mL/kg. All formulations were sterilized prior injection using a sterile 0.2 μm PES filter. Tumor volumes and mice body weights were measured twice per week. Tumor volume (TV) was calculated using the formula: $TV = (width^2 \times length)/2$. As toxicity parameter, body weight, clinical signs and animal behavior were recorded for all mice twice a week. Mice were held in individual ventilated cages (IVC) standardized and controlled environmental conditions. The experiment was terminated when the tumor size exceeded 1.5 cm^3 as ethical endpoint. The work conducted in living mice, at Experimental Pharmacology and Oncology GmbH (Berlin, Germany), is in accordance with the German Animal Welfare Act as well as the UKCCCR (United Kingdom Coordinating Committee on Cancer Research) and all procedures were approved by local authorities (Landesamt für Gesundheit und Soziales, LaGeSo Berlin, Germany) under approval number E0023/23 for preclinical therapeutic experiments.

2.15. Ex vivo tumor analysis

After sacrificing the mice, tumor tissues were excised and embedded in specimen matrix for cryosectioning (Tissue-Tek OCT, Sakura, USA). Cryosections were cut at a thickness of 8 μm and then fixed on glass slides in 80 % (v/v) methanol in water at room temperature, followed by acetone at −20 °C. For immunofluorescence staining of cell proliferation (Ki-67) and apoptosis (cleaved caspase-3), tumor tissues were permeabilized using 0.1 % (v/v) of Triton X-100 in PBS for 10 min. Rabbit anti-Ki-67 (Abcam, UK) primary antibodies were diluted (1:50) in 12 % (w/v) BSA and applied to the permeabilized cryosections for 1 h at room temperature, followed by washing with PBS to remove excess antibody and then incubated with Cy3 anti-rabbit secondary antibody (1:500; Dianova, Germany) for 45 min at room temperature. After another washing step, rabbit anti-cleaved caspase-3 (Abcam, UK) was diluted (1:500) in 12 % (w/v) BSA and added to the slides and incubated for 1 h at room temperature. The excess of antibody was removed by washing with PBS, and sections were incubated for another 45 min at room temperature with Alexa Fluor 488 anti-rabbit secondary antibody (1:500; Dianova, Germany) together with DAPI (4′,6-diamidino-2-phenylindole) nuclei staining (Merck, Germany) diluted 1:500 in 12 % BSA. Antibodies incubation was always performed in a humidified chamber in the dark. Tumor sections were then washed with PBS, mounted with Mowiol 4–88 (anti-fade agent; Carl-Roth, Germany) and glass-covered. Images were acquired using an AxioImager M2 microscopy system with an AxioCamMRm Rev.3 camera (Carl Zeiss AG, Germany). Representative images with a magnification of 100 were acquired from the core ($n = 3$) and periphery (n = 3) per tumor slice (n = 3, per mouse) using the same exposure time settings for each channel for the combined staining. The area fraction (%) of the respective signal was quantified with the AxioVision SE64 Rel. 4.8 software.

2.16. Statistical analysis

Statistical analysis was done using GraphPad prism 9.0 software. Data are expressed as mean ± standard deviation (n = 3; unless stated otherwise). One-way or two-way analysis of variance (ANOVA) with multiple-group comparisons (based on software recommendations) was

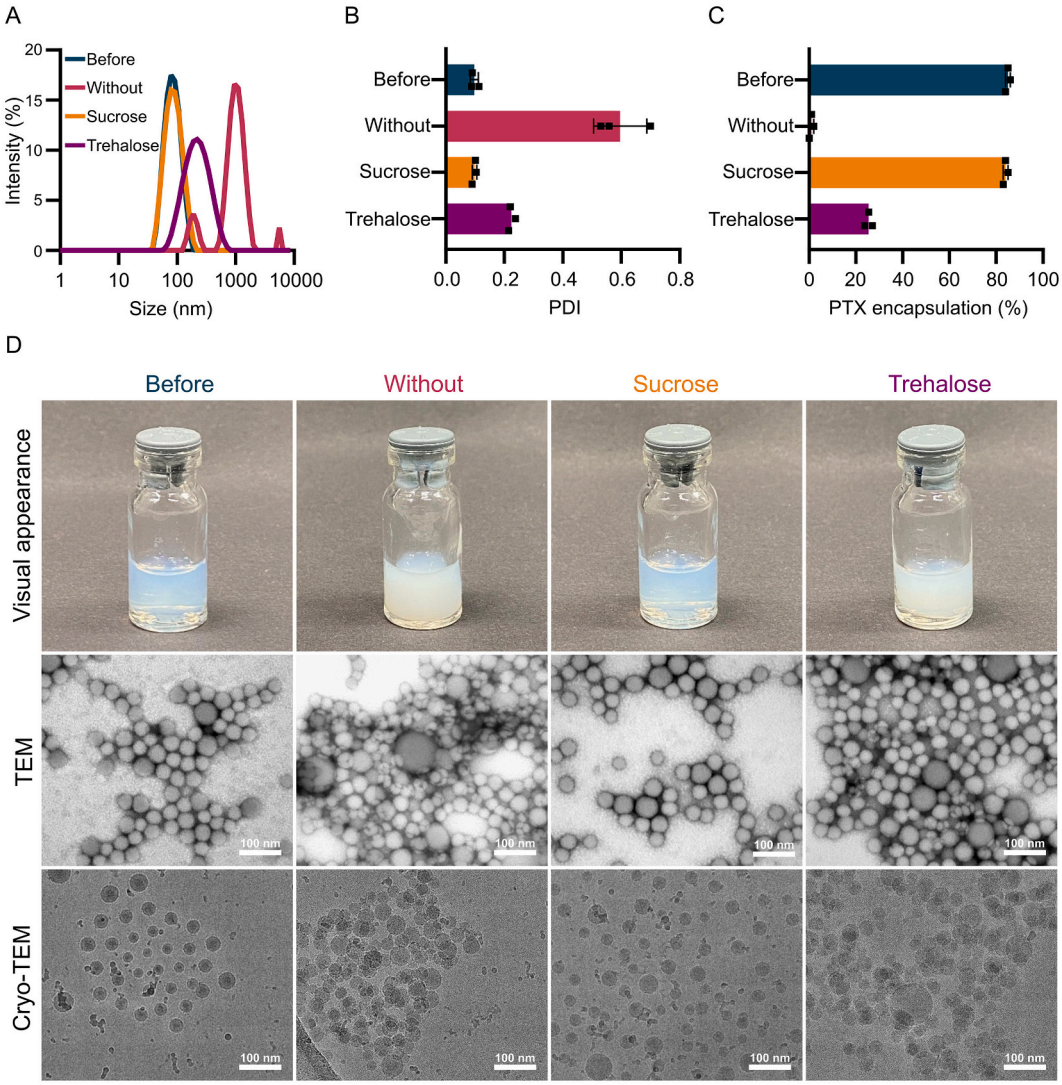

Fig. 2. Effect of sucrose and trehalose on cryoprotection of paclitaxel-loaded [mPEG-*b*-p(HPMAm-Bz)] -based polymeric micelles. A-C) Size distribution (A), polydispersity index (PDI) (B) and paclitaxel (PTX) content (C) of PTX-loaded micelles freshly prepared (before) and after one freeze-thaw (FT) cycle in the absence (without) and presence of disaccharide-based cryoprotectants (sucrose or trehalose) ($n = 3$). **D)** Macroscopic visual appearance and (cryogenic) transmission electron microscopy (TEM and cryo-TEM) images of PTX-loaded micelles after a FT cycle in the absence and presence of sucrose or trehalose. Micelles (1 mL) were prepared at a polymer concentration of 10 mg/mL and PTX feed amount of 1 mg/mL.

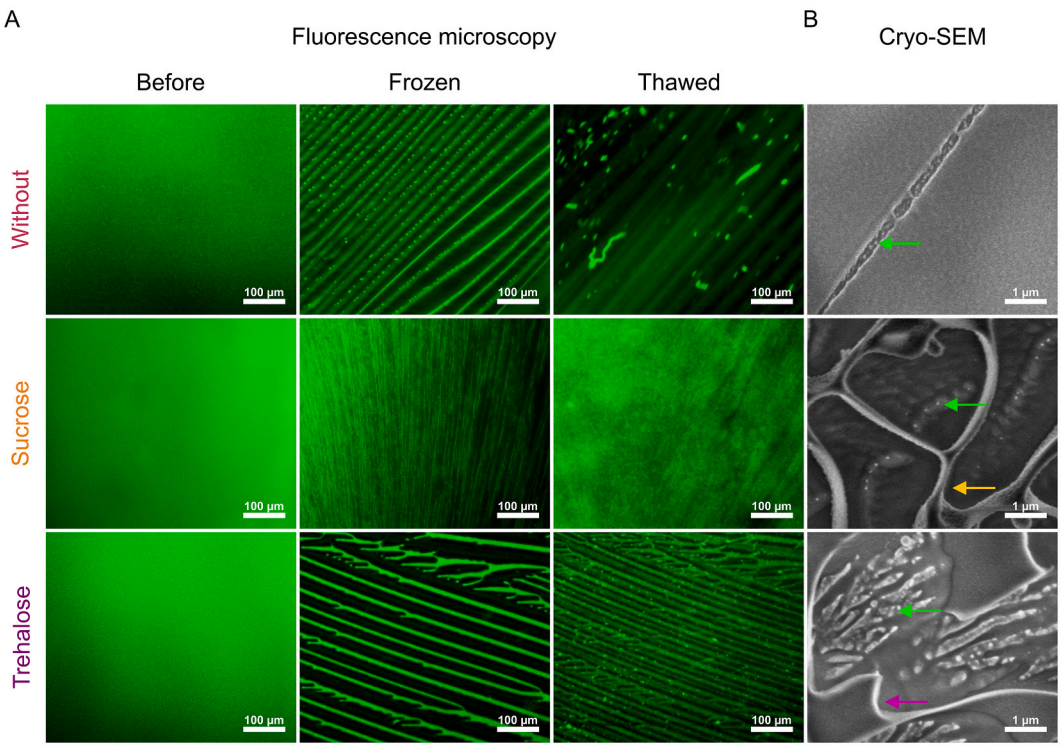

Fig. 3. In-situ freezing microscopy of [mPEG-*b*-p(HPMAm-Bz)]-based polymeric micelles with and without cryoprotectants. A) Fluorescence microscopy images of dry ice-induced in-situ freezing of Cy7-labelled mPEG-*b*-p(HPMAm-Bz) micelles before, during freezing (frozen) and after thawing (thawed), in the absence (without) and presence of cryoprotectants (sucrose or trehalose). **B)** Cryogenic-scanning electron microscopy (cryo-SEM) of frozen fractured mPEG-*b*-p(HPMAm-Bz) micelles (green arrows) in the presence of sucrose (orange arrow) or trehalose (purple arrow) compared to non-cryoprotected micelles (without). (For interpretation of the references to color in this figure legend, the reader is referred to the web version of this article.)

applied, depending on each specific set of data. 0.05 was used as alpha threshold for determining statistical significances, which were considered for p-values < 0.05 (*), $p < 0.01$ (**), $p < 0.001$(***) and $p < 0.0001$ (****).

3. Results and discussion

3.1. Effect of disaccharides on cryoprotection of paclitaxel-loaded micelles

First, we evaluated the impact of the freezing step on the polymeric micelles. To do so, we compared the properties of the formulations before and after a FT cycle. We prepared PTX-loaded mPEG-*b*-p(HPMAm-Bz) micelles (1 mL) using the conventional bench-scale (BS) nanoprecipitation method at a polymer concentration of 10 mg/mL and drug feed amount of 1 mg/mL. Micelles were characterized in terms of size (~80 nm), PDI (≤ 0.1), and PTX encapsulation efficiency (~80 %), and were then diluted with trehalose or sucrose stock solutions to achieve a final CP concentration of 100 mg/mL (i.e., 10 % (w/v)). The concentration of CP was chosen based on what is commonly used in pharmaceutical formulations [12]. The PTX-loaded micelle formulations with and without CP were subjected to a single FT cycle by snap freezing them in liquid nitrogen and were immediately allowed to thaw at room temperature. Micelles without cryoprotective excipients experienced considerable aggregation and destabilization during freezing, as evidenced by the appearance of three micelle populations with distinct sizes in the DLS chromatogram, a significant increase in the PDI values, and the observation of PTX precipitation after thawing (i.e., quantitative loss of encapsulated drug) (Figs. 2A-C). In the case of the formulations containing the two disaccharide-based CPs, the differences are striking. The addition of sucrose proved to be highly effective in cryoprotecting the PTX-loaded micelles, preserving their physicochemical properties (size ~80 nm, PDI ~0.1) and PTX encapsulation efficiency (~80 %) after freeze-thawing (Figs. 2A-C). In contrast, trehalose showed no cryoprotective effect on the polymeric micelles, as observed by the increase in particle size, aggregation (PDI >0.2) and over 75 % loss of encapsulated drug after freeze-thawing. To rule out a concentration-dependent effect, we increased the amount of trehalose in the formulation (20 % (w/v)), but this also resulted in micelle aggregation upon freeze-thawing (Fig. S1).

The finding that sucrose stabilizes the PTX-loaded mPEG-*b*-p(HPMAm-Bz) micelles during freezing was also confirmed by examining their appearance and morphology after thawing by visual inspection and using electron microscopy techniques (TEM and cryo-TEM) (Fig. 2D). Formulations without sucrose or trehalose led to significant micelle destabilization and irreversible aggregation, confirmed by both visual inspection of macroscopic dispersion and the TEM and cryo-TEM images. Consistent with the DLS results (Figs. 2A-B), sucrose preserved the spherical morphology and homogeneity of the particles during freezing and after thawing, while the samples with trehalose showed, both macro- and microscopically, clustering and aggregation, similar to the formulation without any CP (Fig. 2D).

To understand the different performance of trehalose and sucrose and to provide further insights into the cryoprotective effect during the freezing process, we employed optical and electron microscopy techniques. In previous studies, the aggregation of polymeric (PLGA) nanoparticles was visualized using optical fluorescence microscopy by adding labelled polystyrene nanoparticles to the polymeric dispersion [11]. We here extended these efforts by directly labelling our polymeric micelles with a Cy7 fluorescent dye to track them during the freezing step. We synthesized Cy7-functionalized [mPEG-*b*-p(HPMAm-Bz)]-based polymers and used them to visualize the impact of (in-situ) freezing-induced stress on the micelles by fluorescence microscopy.

During the freezing process, phase separation occurs, which results

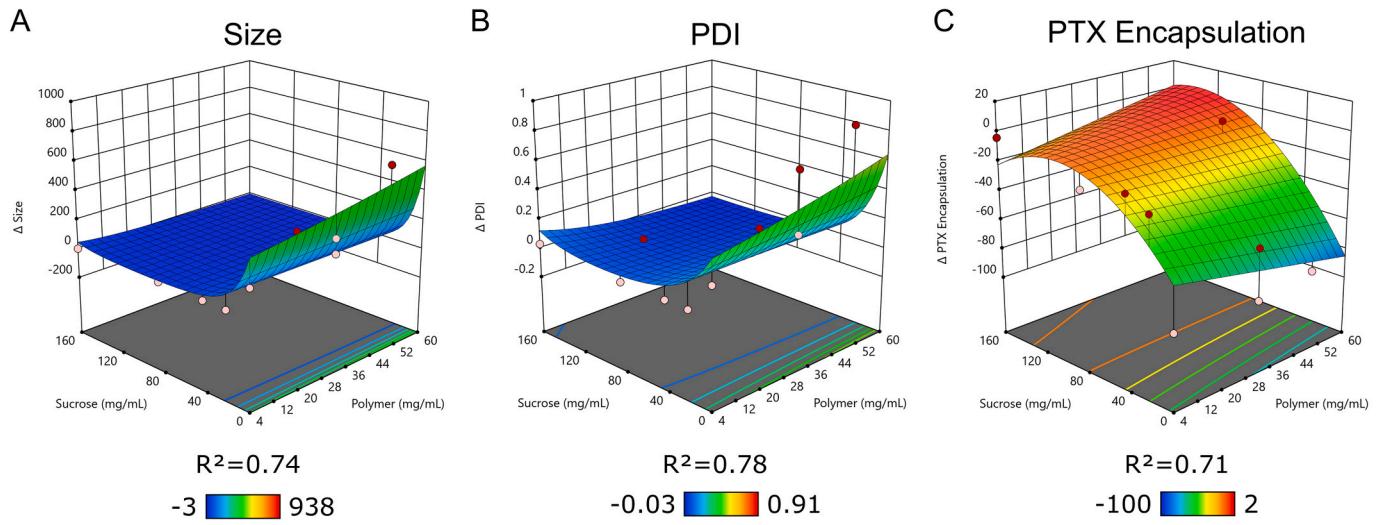

Fig. 4. Effect of formulation composition parameters on the properties of paclitaxel-loaded [mPEG-*b*-p(HPMAm-Bz)]-based polymeric micelles after freeze-thawing. A-C) 3D response-surface plots modelling the effect of formulation composition (i.e., polymer, drug and cryoprotectant (sucrose) concentrations) on the change in hydrodynamic diameter (size) (A), polydispersity (PDI) (B) and paclitaxel (PTX) encapsulation percentage (C) of PTX-loaded micelles after one freeze-thaw (FT) cycle. Each individual data point represents the experimental outcome of one formulation condition. Color bars and values at the bottom of each graph represent absolute differences in size, PDI and PTX encapsulation. Each individual experiment is detailed in Table S1. Concentration ranges used to prepare the different micelles are: polymer, 4–60 mg/mL; drug feed amount, 1–7.5 mg/mL; and sucrose, 0–160 mg/mL. The quality assessment of the models is provided in Table S2.

in a frozen fraction composed of ice and another unfrozen fraction that remains stable between these frozen fractions, and which contains the nanoparticles along with other components such as buffer, different excipients, unencapsulated drug, and water molecules adsorbed onto the surface of the particles [13,36]. Using in-situ freezing fluorescence microscopy (Fig. 3A), we observed that ice crystals (dark regions) started to form unidirectionally across the slide upon dry ice-induced freezing due to the existing temperature gradient, while the unfrozen fraction containing the Cy7-labelled micelles (green regions) remained squeezed between the formed ice-crystals. All the formulations were homogeneous before freezing but behaved differently after the FT cycle. Without CP, the ice-induced phase separation and mechanical stress caused aggregation of the micelles and formation of fiber-like polymer aggregates, as evidenced by the intense and non-homogeneous fluorescence signal observed after thawing. In the presence of sucrose, phase separation was reduced during freezing, and the micelles were more homogenously distributed within the frozen sample, which prevented aggregation and preserved particle distribution after thawing. Instead, trehalose did not prevent phase separation of the micelles under these experimental conditions and exposed them to the solid (ice)-liquid (unfrozen) interface, and hence, to a higher mechanical stress that led to particle clustering and aggregation.

Due to the limited resolution of optical microscopes, accurately visualizing the individual particles and their location within the confined unfrozen fractions during freezing is challenging. We employed cryo-SEM to further explore the impact of freezing-induced phase separation on micelle aggregation in the presence of CPs. As shown in Fig. 3B (green arrow), micelles were found in close contact with each other when frozen in the absence of the CPs. The addition of sucrose resulted in the formation of an entwined microstructure upon freezing with the particles confined in it (orange arrow, Fig. 3B); effectively isolating them from the ice and from clustering with neighboring particles. In the case of trehalose, cryo-SEM images also showed the formation of similar micro-structured chambers upon freezing, albeit to a lesser extent (purple arrow, Fig. 3B). Yet, with trehalose as CP, the particles were more aggregated and heterogeneously distributed within the frozen sample (green arrow, Fig. 3B). It has been reported that trehalose forms stronger hydrogen bonds than sucrose with heteroatoms on the surface of nanoparticles [12] (for the mPEG-*b*-p(HPMAm-Bz) micelles, the oxygen atom present in the hydrophilic PEG shell); and, therefore, that it can replace the adsorbed water molecules more effectively. This has made trehalose an effective CP for various nanoparticle types [12,37], including polymeric micelles like core-crosslinked HPMA-based micelles [38]. However, our findings demonstrate that the water replacement of trehalose is not always effective, and that the cryoprotective performance of (disaccharide-based) CPs is highly dependent not only on the type of nanoparticle but also on the specific (polymer) composition. This has been corroborated in micelles based on methoxy poly(ethylene glycol)–poly(hexyl-lactide) block copolymers, where sucrose also outperformed trehalose in cryoprotection efficiency [39], together indicating that more in-depth analyses are needed in the future to fully understand the different performance of CPs at the molecular level.

3.2. *Effect of formulation composition on cryoprotection of paclitaxel-loaded polymeric micelles*

Based on the above results, sucrose was selected as the CP for the mPEG-*b*-p(HPMAm-Bz) polymeric micelles. Sucrose is also used as a cryoprotective excipient in the formulation of the recently approved mRNA LNP-based COVID-19 vaccines. For instance, the Spikevax COVID-19 vaccine uses sucrose at a concentration of 87 mg/mL, while the Comirnaty vaccine contains 100 mg/mL [10]. These two examples illustrate that the amount of CP is adjusted for each specific formulation composition. Additionally, several studies have shown that the mass ratio of nanoparticles to CP can strongly impact the cryoprotective effectiveness of CPs [12,14]. Our initial screening experiments for the micelles were done on formulations prepared at a polymer concentration of 10 mg/mL and with a PTX feed amount of 1 mg/mL. Given that commercially available PTX formulations contain around 6 mg/mL of PTX [40], and that previous preclinical studies of our micelle platform have used polymer concentrations of 30 mg/mL [25], we set out to evaluate the influence of different polymer and drug concentrations on the cryoprotective performance of sucrose, and to identify the minimum required sucrose concentration for optimal cryopreservation of the micelles.

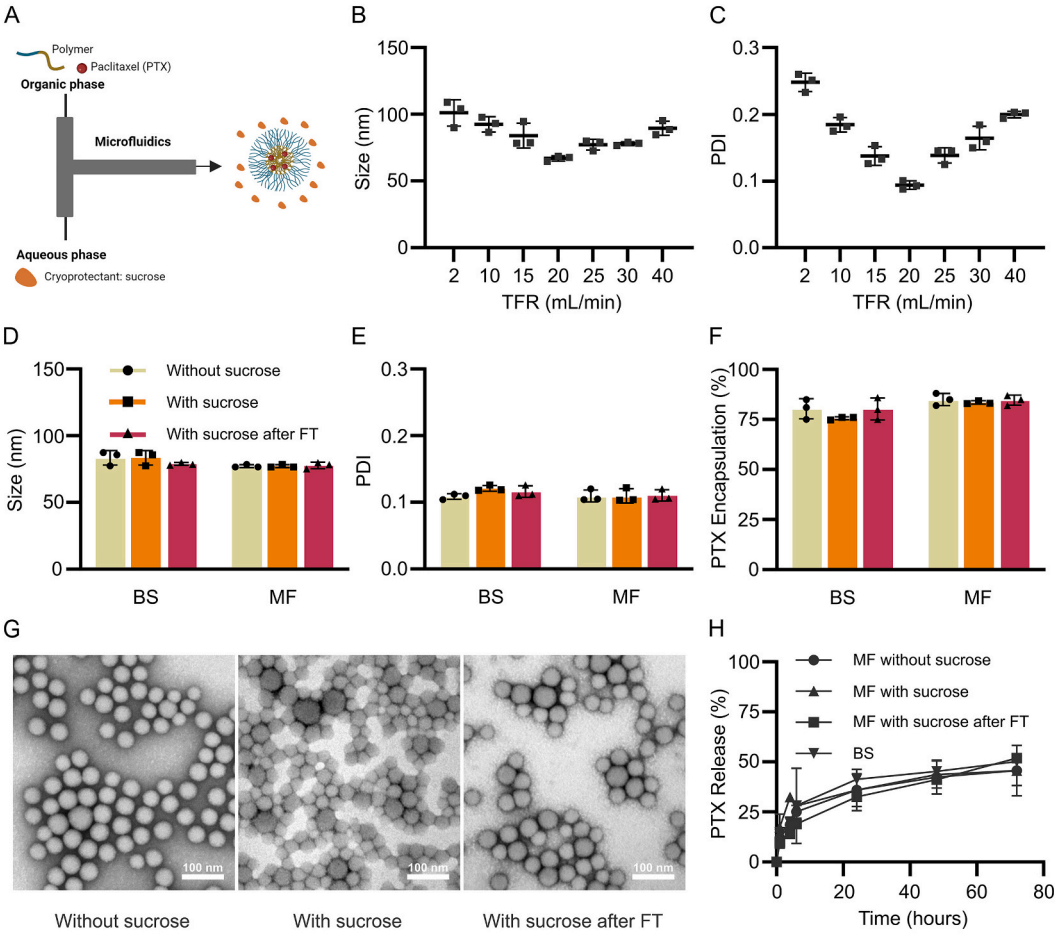

Fig. 5. Microfluidic formulation of paclitaxel-loaded [mPEG-*b*-p(HPMAm-Bz)]-based polymeric micelles containing sucrose as a cryoprotectant. A) Schematic design of the microfluidic (MF) setup. Briefly, the organic phase containing the polymer and paclitaxel (PTX) drug in THF was pumped against the aqueous phase (with or without containing sucrose). **B-C)** Size (B) and polydispersity index (PDI) (C) of empty micelles prepared via MF mixing at different total flow rates (TFR). **D-F)** Size (D), PDI (E), PTX encapsulation efficiency (F) of PTX-loaded micelles prepared via MF mixing, without or with sucrose in the aqueous phase, and before and after a freeze-thaw (FT) cycle, as compared to the micelles prepared using the conventional bench-scale (BS) method. **G-H)** Transmission electron microscopy images (G) and drug release profiles (H) of PTX-loaded micelles prepared via MF mixing, without or with sucrose in the aqueous phase, and after FT of the latter. Drug release profile of the standard PTX-micelle formulation without sucrose and prepared using the BS nanoprecipitation method was also added for comparison. All the micelles were prepared using a polymer concentration of 30 mg/mL and PTX feed amount of 7.5 mg/mL. For the sucrose-containing formulations, a final sucrose concentration of 80 mg/mL was used. Statistical analyses ($n = 3$) were done using two-way ANOVA with Tukey's multiple comparison test (D-F and H). No statistical differences were found regarding micelle properties (D-F and H) before and after FT or with and without the addition of sucrose.

We designed a systematic study with varying amounts of polymer, drug and CP based on a design of experiments (DoE) approach and evaluated the impact of different concentrations on three key CQAs before and after freeze-thawing: size, PDI, and amount of encapsulated drug. Formulations with polymer concentrations ranging from 4 to 60 mg/mL and drug (PTX) feed amounts from 1 to 7.5 mg/mL were prepared, and each was diluted by 20 % with different sucrose stock solutions to achieve a final sucrose concentration ranging from 0 to 160 mg/mL (Table S1). After a single FT cycle, we characterized the formulations and compared their properties with those before freezing. The resulting mathematical models representing the effect of the different compositions on the micelle properties were of good quality, based on the different coefficients of determination (Fig. 4 and Table S2).

In line with previous results, micelle size and PDI substantially increased after freeze-thawing in the absence of sucrose, whereas the addition of the sucrose as CP minimized the change in these properties (Figs. 4A-B). The polymer concentration showed minimal impact on micelle size, while it had a slight effect on the dispersity of the formulations after the FT cycle, especially when the concentration of sucrose was below 40 mg/mL. This is likely because high polymer concentrations lead to a large number of self-assembly nucleation points during freezing, thereby increasing the probability of particle aggregation if the concentration of CP is too low to keep the particles isolated [29]. Based on the obtained models and the DoE-based multivariate analysis, a final sucrose concentration of 40 mg/mL was identified to be sufficient to cryopreserve the physicochemical properties (size and PDI) of the PTX-loaded [mPEG-*b*-p(HPMAm-Bz)]-based micelles within the assayed polymer concentration range. However, our aim was to determine the minimum amount of sucrose needed to also retain the drug encapsulated within the micelles after freeze-thawing. Regarding PTX encapsulation, analysis of the obtained models indicated that the optimal sucrose concentrations for the micelle formulations used here range between 80 and 120 mg/mL, depending on the polymer concentration (Fig. 4C). As mentioned before, since preclinical evaluation of these micelles was performed at a polymer concentration of 30 mg/mL [25], 80 mg/mL would then be the minimum concentration of sucrose required for effective cryoprotection of our formulation, which is in the range of the amounts used in other approved nano-pharmaceuticals [10].

Validation of these conclusions was done by preparing fresh micelles at a polymer concentration of 30 mg/mL, PTX feed amount of 7.5 mg/mL and a final sucrose concentration of either 20, 40, or 80 mg/mL (Fig. S2). We found that the pharmaceutical properties were effectively

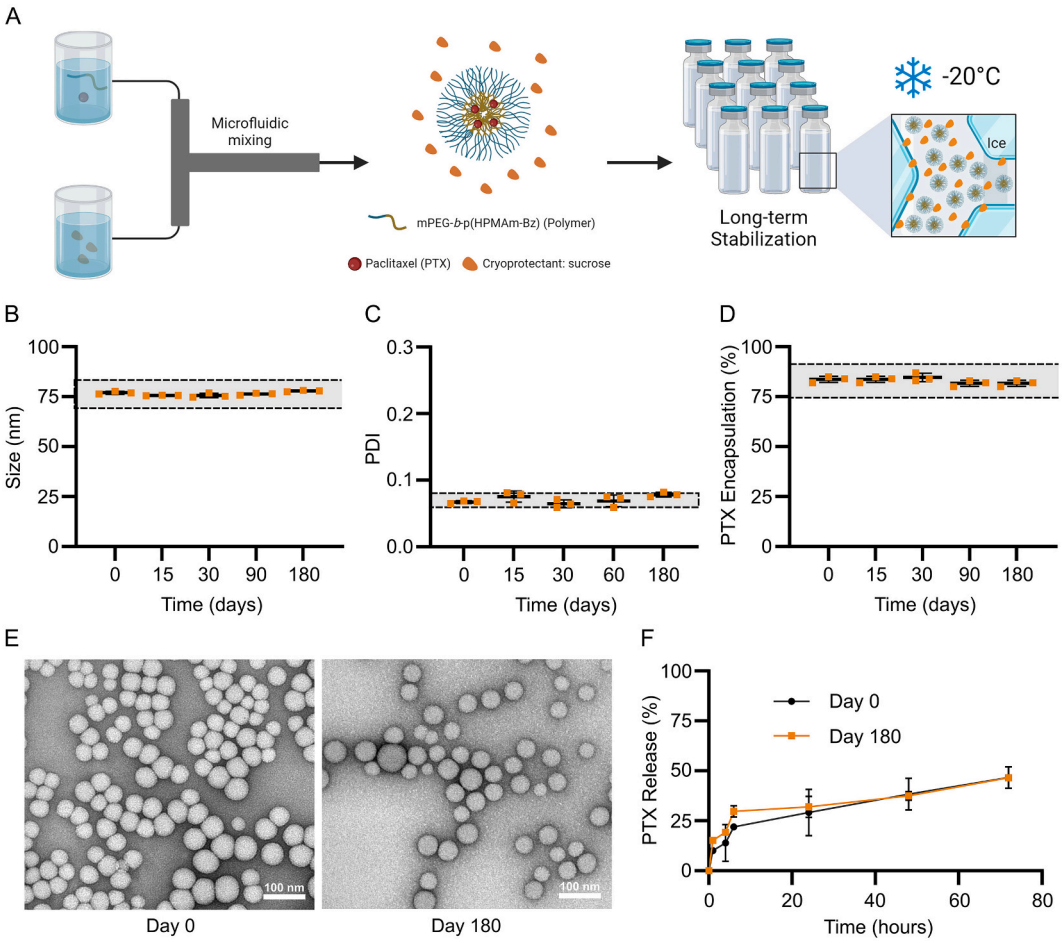

Fig. 6. Long-term stability evaluation of microfluidic-formulated paclitaxel-loaded polymeric micelles with sucrose as cryoprotectant. A) Schematic setup of continuous-flow microfluidic (MF) production of paclitaxel-loaded micelles with sucrose dissolved in the aqueous phase. **B-D)** Size (B), polydispersity index (PDI) (C) and PTX encapsulation efficiency (D) of cryopreserved PTX-loaded micelles stored at −20 °C, monitored for 6 months (*note*: area between the dashed lines refers to ±10 % of the value at day 0 (fresh formulation, before freezing)). **E)** Transmission electron microscopy images of PTX-loaded micelles formulated using MF in the presence of sucrose as a cryoprotectant on day 0 (fresh) and after 180 days of being stored frozen at −20 °C. **F)** Cumulative drug release profile of cryopreserved PTX-micelles after 180 days of storage, frozen, at −20 °C compared to the freshly prepared formulation (day 0). Polymer concentration used to prepare the 10 mL-micelle batch: 30 mg/mL; PTX feed amount: 7.5 mg/mL; and sucrose concentration: 80 mg/mL. Statistical analyses ($n = 3$) were done using one-way (B-D) and two-way ANOVA analyses (F) with Tukey's multiple comparison test. No statistical differences were found regarding micelle properties (B-D, F) before and after storage at −20 °C in any case.

preserved after a FT cycle only for the formulation containing 80 mg/mL of sucrose. Overall, the goodness-of-fit, significance and representativeness values of the DoE-based models indicated therefore a good mathematical adjustment of the experimental data ($R^2 > 0.7$ and p-values <0.0001 in all cases), thus contributing to profile the effect of the formulation composition on the cryoprotection efficacy. In the future, additional runs can help further improve model quality, particularly when more accurate predictions about changes in size and PDI are required.

3.3. *Microfluidic formulation of paclitaxel-loaded polymeric micelles with sucrose as cryoprotectant*

After selection of sucrose as the CP and its optimal concentration for effective cryopreservation, the use of MF mixing technologies as a proof-of-concept framework for continuous-flow production of the PTX-loaded micelles was explored. In this context, we also aimed to eventually integrate the addition of sucrose as the cryoprotective excipient into a single MF-based micelle formulation step (Fig. 5A). In the first step, we studied the effect of total flow rate (TFR) as a process parameter on the properties of the non-loaded micelles. To do so, we used a MF-chip with a zig-zag (ZZ) mixing pattern (Fig. S3A), which had previously shown promise in formulating liposomes and polymeric nanoparticles [33]. Both the polymer and the drug were dissolved in the organic phase (THF) and pumped against water at a fixed 1:1 (aqueous: organic phase) flow rate ratio, in line with the solvent proportions used for the BS nanoprecipitation method. Different TFRs, ranging from 2 to 40 mL/min were investigated (Figs. 5B-C). Overall, micelles were formed in all cases, with variations in size and PDI values, in line with previous findings [41]. While TFRs between 10 and 30 mL/min rendered homogeneous particles (PDI below 0.2), TFR of 20 mL/min resulted in micelles with sizes around 70 nm and the lowest PDI value (about 0.1), comparable to the BS method. To assess the robustness of the MF formulation of the micelles, we corroborated the results with another chip with a different mixing pattern (split and recombine (SR), Fig. S3A), which has been reported to require longer times than the ZZ chip to achieve complete mixing of the two solvents [33]. Micelles were also successfully formulated in the SR chip following similar conditions, and we saw a similar trend in PDI to that found for the ZZ chip upon different TFRs, with slight differences only in size (particularly at TFRs ≥10 mL/min) (Figs. S3B-C).

Then, we investigated the use of the MF setup and the optimized parameters to prepare PTX-loaded micelles. As shown in Figs. 5D-F, the drug-loaded micelles had comparable formulation properties (size, PDI,

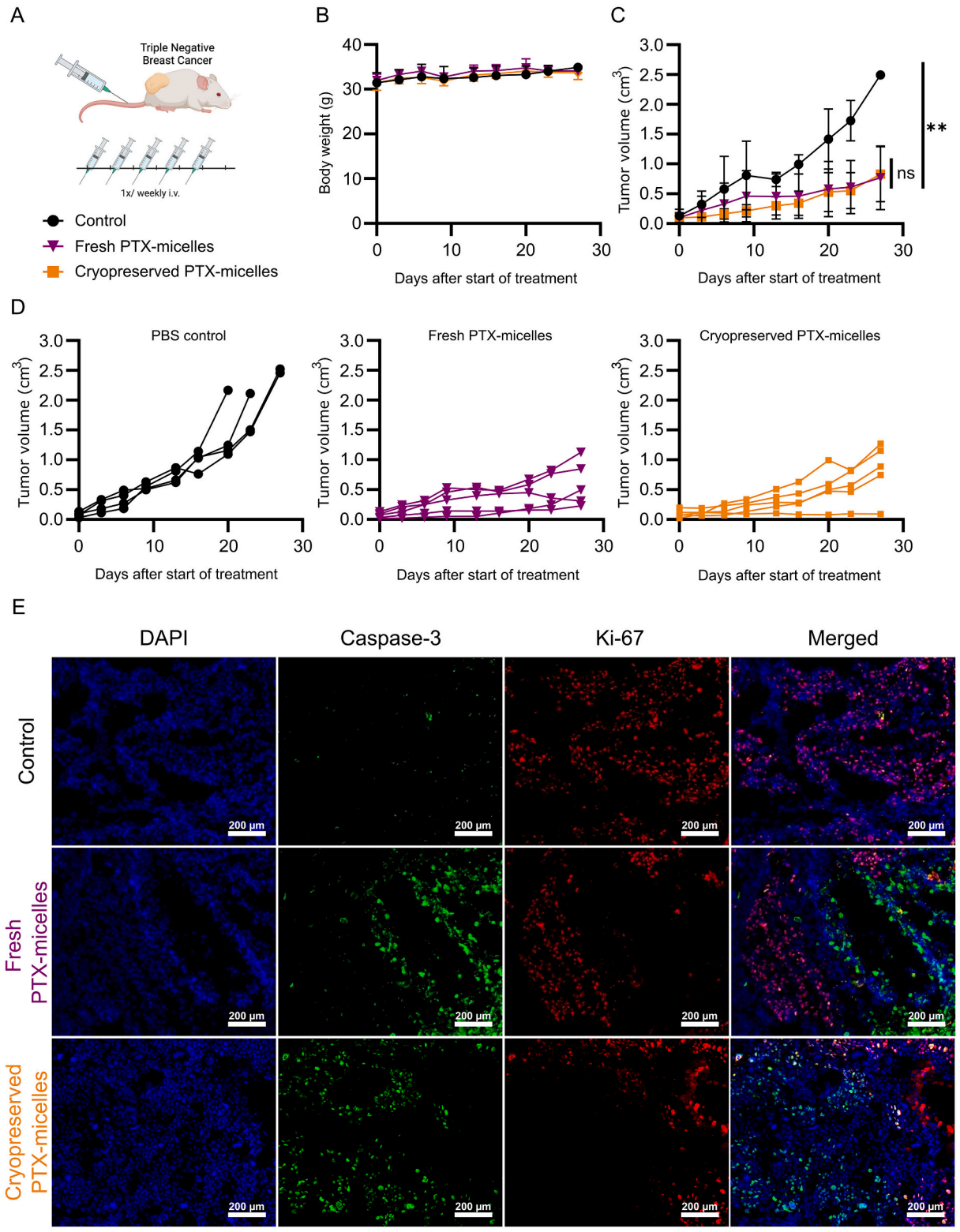

Fig. 7. Therapeutic performance of cryopreserved paclitaxel-loaded polymeric micelles as compared to freshly prepared formulations. A) Patient-derived triple-negative breast cancer specimens (PDX, Ma14986) were xenografted in the fat-pad of female NMRI nu/nu mice. Cryopreserved (and thawed prior to injection) vs. fresh paclitaxel (PTX)-loaded micelles were administered at a PTX dose of 30 mg/kg body weight. Once tumors reached 0.1 cm^3 ($n = 5$ per treatment group), five intravenous injections were given, once weekly. **B)** Mouse body weight over the course of treatment. **C)** Mean tumor volumes based on caliper measurements for frozen (cryopreserved) and fresh PTX-formulations vs. PBS control. **D**) Individual tumor growth curves for each treatment group (PBS, and fresh and cryopreserved PTX-micelles). **E**) Ex vivo fluorescence microscopy images showing activated caspase-3 (apoptosis) and Ki-67 (proliferation) positive tumor cells. Nuclei were counterstained using DAPI. Statistical analyses were done using two-way ANOVA analysis with Tukeý s multiple comparison test (p-values > 0.05 (ns), $p < 0.01$ (**)).

and PTX encapsulation efficiency) with those prepared via BS nanoprecipitation. In order to reduce the number of formulation steps and eventually contribute to streamlining micelle preparation, the possibility of adding sucrose in the aqueous phase inlet before the MF mixing was explored. Using the optimized formulation composition, PTX-loaded micelles were prepared by dissolving the polymer (30 mg/mL) and the drug (7.5 mg/mL PTX) in the organic phase (THF), and sucrose (80 mg/mL) in the aqueous phase, using both MF and BS method. The presence of sucrose in the aqueous inlet did not impact the physicochemical properties (size or PDI) or drug encapsulation efficiency of the MF-formulated PTX-loaded micelles, and these properties were effectively retained after a FT cycle (Figs. 5D-G). No differences in size, PDI or drug encapsulated were observed either between the micelles prepared via BS and MF. Besides enhancing control over formulation properties, MF mixing also resulted in high batch-to-batch reproducibility (Fig. S4). Importantly, the drug release profiles (at 37 °C in sink conditions) of the MF-formulated PTX-loaded micelles containing sucrose before and after FT were not significantly different between each other, and comparable to the fresh BS formulation (Fig. 5H). Altogether, the integrated MF-setup enable faster formulation of larger volumes of PTX-loaded micelles with sucrose as cryoprotective excipient in a single step, which can be practically useful towards future large-scale continuous-flow production of the micelle formulations.

3.4. Evaluation of long-term stability of paclitaxel-loaded micelles

We have shown that PTX-loaded [mPEG-*b*-p(HPMAm-Bz)]-based micelles can be successfully formulated with sucrose using a MF-based continuous-flow setup, and that these are stable after freeze-thawing upon snap-freezing procedures. However, snap-freezing protocols using liquid nitrogen are not cost-effective at industrial-scale settings. Additionally, the tested cryoprotection conditions involve vitrification of the formulation at temperatures below its glass transition temperature (Tg'), therefore also raising storage costs. Thus, we subsequently evaluated whether sucrose could cryopreserve the micelles during (long-term) storage without requiring temperatures below their Tg' (−35 °C, Fig. S5), which would allow for more easily accessible and cost-effective storage conditions [42,43]. To test this, we formulated a 10 mL-batch of PTX-loaded micelles using the MF-mixing technology and with sucrose as a cryoprotective excipient, and we evaluated the stability of the formulation stored at −20 °C for several months (Fig. 6A).

As shown in Figs. 6B-D, the physicochemical properties and PTX content of the formulations remained stable over time, without any sign of aggregation or drug precipitation during storage for 6 months, thereby confirming successful cryoprotection of PTX-loaded micelles at −20 °C. TEM images of the micelles at day 0 (fresh) and after 180 days storage at −20 °C corroborated these findings and showed the preservation of the spherical morphology and homogeneity of the particles (Fig. 6E). Moreover, the PTX release profile of the thawed micelles after being stored frozen at −20 °C for 180 days was comparable to that of the freshly prepared counterparts (Fig. 6F). The results therefore confirm that MF-formulated PTX-loaded micelles in the presence of sucrose are stable and can be stored frozen at −20 °C for at least 6 months.

Finally, to validate that beyond the assessed formulation properties (i.e., size, size distribution, drug content and drug release; as potential CQAs for the micelles), also the therapeutic performance and tolerability of the frozen nanomedicine formulations could be efficiently preserved, we carried out a comparative in vivo study. To this end, frozen cryoprotected PTX-micelles (after being stored at −20 °C, with sucrose as CP) were shipped to a partner laboratory (Experimental Pharmacology and Oncology GmbH (EPO), in Berlin) and compared head-to-head with formulations freshly prepared on-site (Figs. 7 and S6). We used a patient-derived triple-negative breast cancer xenograft (PDX) model and administered both PTX-formulations intravenously at a 30 mg/kg PTX dose once per week (Fig. 7A). Figs. 7B-7D show that the cryopreserved and freshly-prepared PTX-loaded micelles exhibited comparable tumor growth inhibition and good tolerability based on body weight, with no statistically significant differences between both treatment groups, in line with previous findings on the effective preservation of the pharmaceutical properties of the micelles. To validate the in vivo results, we used tumor cryosections and performed immunofluorescence stainings of proliferation (Ki-67) and apoptosis (cleaved caspase-3), again confirming preservation of preclinical performance after freezing (Figs. 7E and S7). Together, the comparable biocompatibility and similar therapeutic performance confirm the tested pharmaceutical properties as relevant CQAs for the PTX-loaded micelles, as well as demonstrate the long-term storage and shipping stability of frozen π electron-stabilized PTX-micelle formulations containing sucrose as a cryoprotective excipient.

4. Conclusion

We show that freezing-induced phase separation triggers [mPEG-*b*-p(HPMAm-Bz)]-based polymeric micelle aggregation and destabilization, and we demonstrate that this can be prevented with the addition of sucrose (but not trehalose) as a cryoprotectant. Systematic evaluation of different composition parameters of the formulation revealed that sucrose concentration plays a more significant role in preservation of the micelle properties upon freezing than polymer or drug content. We also successfully formulated PTX-loaded [mPEG-*b*-p(HPMAm-Bz)] micelles using microfluidics in the presence of 8 % (w/v) of sucrose as a cryoprotective excipient. Cryoprotected micelles could be successfully stabilized at cryogenic temperatures (−20 °C) for at least 6 months. Frozen cryoprotected micelles preserved their pharmaceutical properties and therapeutic performance upon storage and shipment, showing equivalent efficacy and tolerability as compared to the freshly prepared PTX-micelle formulation. Overall, this work not only promotes pharmaceutical development of the polymeric micelles, but also paves the way towards exploring other relevant long-term stabilization technologies such as lyophilization (freeze-drying) in the future. Our findings furthermore underscore the importance of evaluating aspects such as continuous-flow preparation and long-term stability at early developmental stages, in order to facilitate industrial-scale nanomedicine manufacturing and clinical translation.

CRediT authorship contribution statement

Rahaf Mihyar: Writing – original draft, Visualization, Methodology, Investigation, Formal analysis, Conceptualization. **Armin Azadkhah Shalmani:** Writing – review & editing, Supervision, Investigation, Formal analysis, Conceptualization. **Viktor Wildt:** Investigation, Formal analysis. **Maryam Sheybanifard:** Investigation, Formal analysis. **Alec Wang:** Writing – review & editing, Resources, Investigation. **Jan-Niklas May:** Writing – review & editing, Funding acquisition, Formal analysis. **Saba Shahzad:** Resources, Methodology, Investigation, Formal analysis. **Eva Miriam Buhl:** Writing – review & editing, Resources, Methodology, Investigation. **Stephan Rütten:** Resources, Methodology, Investigation. **Diana Behrens:** Writing – review & editing, Resources, Investigation. **Wolfgang Walther:** Writing – review & editing, Resources, Investigation. **Mattia Tiboni:** Writing – review & editing, Resources. **Luca Casettari:** Writing – review & editing, Resources. **Johannes F. Buyel:** Writing – review & editing, Software, Methodology, Formal analysis, Data curation. **Cristianne J.F. Rijcken:** Writing – review & editing. **Wim E. Hennink:** Writing – review & editing. **Saskia von Stillfried:** Writing – review & editing, Supervision. **Fabian Kiessling:** Writing – review & editing, Funding acquisition. **Yang Shi:** Writing – review & editing, Funding acquisition, Formal analysis. **Josbert M. Metselaar:** Writing – review & editing, Supervision, Funding acquisition. **Twan Lammers:** Writing – review & editing, Supervision, Project administration, Funding acquisition, Conceptualization. **Quim Peña:** Writing – review & editing, Visualization, Supervision, Project administration, Formal analysis, Conceptualization.

Data availability

Data will be made available on request.

Acknowledgments

The authors gratefully acknowledge support from the German Federal Ministry of Research and Education (BMBF: Gezielter Wirkstofftransport, PP-TNBC, Project No. 16GW0319K), the German Research Foundation (DFG: GRK/RTG2735 (project number 331065168); LA2937/4-1; SH1223/1-1; SFB1066), the European Research Council (ERC: ERC-CoG Meta-Targeting (864121)), and the Erasmus Mundus Joint Master Degree of the NANOMED Program (scholarship to Rahaf Mihyar). The electron microscopy time granted by the Life Science Facility at the Ernst-Ruska center at the Forschungszentrum Jülich is also acknowledged. The authors would like to thank Dr. Rostislav Vinokur (DWI – Leibniz Institute for Interactive Materials, Aachen, Germany) for support in DSC, Dr. Lars Winkler (Experimental Pharmacology and Oncology GmbH, Berlin, Germany) for support in DLS measurements, Britta Büttner (Experimental Pharmacology and Oncology GmbH, Berlin) for experimental support during the in vivo study, and Elena Rama and Susanne Koletnik (Institute for Experimental Molecular Imaging, Aachen, Germany) for assistance with the ex vivo microscopy analysis.

Appendix A. Supplementary data

Supplementary data to this article can be found online at https://doi.org/10.1016/j.jconrel.2024.08.041.

References

[1] J.M. Metselaar, T. Lammers, Challenges in nanomedicine clinical translation, drug Deliv, Transl. Res. 10 (2020) 721–725, https://doi.org/10.1007/s13346-020-00740-5.
[2] J.I. Hare, T. Lammers, M.B. Ashford, S. Puri, G. Storm, S.T. Barry, Challenges and strategies in anti-cancer nanomedicine development: an industry perspective, Adv. Drug Deliv. Rev. 108 (2017) 25–38, https://doi.org/10.1016/j.addr.2016.04.025.
[3] L. Schoenmaker, D. Witzigmann, J.A. Kulkarni, R. Verbeke, G. Kersten, W. Jiskoot, D.J.A. Crommelin, mRNA-lipid nanoparticle COVID-19 vaccines: structure and stability, Int. J. Pharm. 601 (2021), https://doi.org/10.1016/j.ijpharm.2021.120586.
[4] L. Kudsiova, A. Lansley, G. Scutt, M. Allen, L. Bowler, S. Williams, S. Lippett, S. Stafford, M. Tarzi, M. Cross, M. Okorie, Stability testing of the Pfizer-BioNTech BNT162b2 COVID-19 vaccine: a translational study in UK vaccination centres, BMJ Open Science 5 (2021) e100203, https://doi.org/10.1136/bmjos-2021-100203.
[5] D.J.A. Crommelin, T.J. Anchordoquy, D.B. Volkin, W. Jiskoot, E. Mastrobattista, Addressing the cold reality of mRNA vaccine stability, J. Pharm. Sci. 110 (2021) 997–1001, https://doi.org/10.1016/j.xphs.2020.12.006.
[6] M. Sheybanifard, L.P.B. Guerzoni, A. Omidinia-Anarkoli, L. De Laporte, J. Buyel, R. Besseling, M. Damen, A. Gerich, T. Lammers, J.M. Metselaar, Liposome manufacturing under continuous flow conditions: towards a fully integrated set-up with in-line control of critical quality attributes, Lab Chip 23 (2022) 182–194, https://doi.org/10.1039/d2lc00463a.
[7] T.A. Bauer, J. Schramm, F. Fenaroli, S. Siemer, C.I. Seidl, C. Rosenauer, R. Bleul, R. H. Stauber, K. Koynov, M. Maskos, M. Barz, Complex structures made simple – continuous flow production of Core Cross-linked polymeric micelles for paclitaxel pro-drug-delivery, Adv. Mater. 35 (2023), https://doi.org/10.1002/adma.202210704.
[8] J. Bresseleers, M. Bagheri, G. Storm, J.M. Metselaar, W.E. Hennink, S. A. Meeuwissen, J.C.M. Van Hest, Scale-up of the manufacturing process to produce docetaxel-loaded mPEG- b-p(HPMA-Bz) block copolymer micelles for pharmaceutical applications, Org. Process. Res. Dev. 23 (2019) 2707–2715, https://doi.org/10.1021/acs.oprd.9b00387.
[9] K.N. Kafetzis, N. Papalamprou, E. McNulty, K.X. Thong, Y. Sato, A. Mironov, A. Purohit, P.J. Welsby, H. Harashima, C. Yu-Wai-Man, A.D. Tagalakis, The effect of Cryoprotectants and storage conditions on the transfection efficiency, Stability, and Safety of Lipid-Based Nanoparticles for mRNA and DNA Delivery, Adv Healthc Mater 18 (2023) e2203022, https://doi.org/10.1002/adhm.202203022.
[10] S. Meulewaeter, G. Nuytten, M.H.Y. Cheng, S.C. De Smedt, P.R. Cullis, T. De Beer, I. Lentacker, R. Verbeke, Continuous freeze-drying of messenger RNA lipid nanoparticles enables storage at higher temperatures, J. Control. Release 357 (2023) 149–160, https://doi.org/10.1016/j.jconrel.2023.03.039.
[11] L. Niu, J. Panyam, Freeze concentration-induced PLGA and polystyrene nanoparticle aggregation: imaging and rational design of lyoprotection, J. Control. Release 248 (2017) 125–132, https://doi.org/10.1016/j.jconrel.2017.01.019.
[12] P. Fonte, S. Reis, B. Sarmento, Facts and evidences on the lyophilization of polymeric nanoparticles for drug delivery, J. Control. Release 225 (2016) 75–86, https://doi.org/10.1016/j.jconrel.2016.01.034.
[13] M.A. Mensink, H.W. Frijlink, K. van der Voort Maarschalk, W.L.J. Hinrichs, How sugars protect proteins in the solid state and during drying (review): mechanisms of stabilization in relation to stress conditions, Eur. J. Pharm. Biopharm. 114 (2017) 288–295, https://doi.org/10.1016/j.ejpb.2017.01.024.
[14] E. Trenkenschuh, W. Friess, Freeze-drying of nanoparticles: how to overcome colloidal instability by formulation and process optimization, Eur. J. Pharm. Biopharm. 165 (2021) 345–360, https://doi.org/10.1016/j.ejpb.2021.05.024.
[15] F. Susa, G. Bucca, T. Limongi, V. Cauda, R. Pisano, Enhancing the preservation of liposomes: the role of cryoprotectants, lipid formulations and freezing approaches, Cryobiology 98 (2021) 46–56, https://doi.org/10.1016/j.cryobiol.2020.12.009.
[16] D. Guimarães, J. Noro, C. Silva, A. Cavaco-Paulo, E. Nogueira, Protective effect of saccharides on freeze-dried liposomes encapsulating drugs, Front. Bioeng. Biotechnol. 7 (2019), https://doi.org/10.3389/fbioe.2019.00424.
[17] T. Starciuc, B. Malfait, F. Danede, L. Paccou, Y. Guinet, N.T. Correia, A. Hedoux, Trehalose or sucrose: which of the two should be used for stabilizing proteins in the solid state? A Dilemma Investigated by In Situ Micro-Raman and Dielectric Relaxation Spectroscopies During and After Freeze-Drying, J. Pharm. Sci. 109 (2020) 496–504, https://doi.org/10.1016/j.xphs.2019.10.055.
[18] C. Jong-Yuh, P. van de Wetering, H. Talsma, D.J.A. Crommelin, W.E. Hennink, Freeze-drying of poly((2-dimethylamino)ethyl methacrylate)-based gene delivery systems, Pharm. Res. 14 (1997) 1838–1841, https://doi.org/10.1023/A:1012164804441.
[19] A.M. Alkilany, S.R. Abulateefeh, K.K. Mills, A.I. Bani Yaseen, M.A. Hamaly, H. S. Alkhatib, K.M. Aiedeh, J.W. Stone, Colloidal stability of citrate and mercaptoacetic acid capped gold nanoparticles upon lyophilization: effect of capping ligand attachment and type of cryoprotectants, Langmuir 30 (2014) 13799–13808, https://doi.org/10.1021/la504000v.
[20] J. Kopeček, P. Kopečková, HPMA copolymers: origins, early developments, present, and future, Adv. Drug Deliv. Rev. 62 (2010) 122–149, https://doi.org/10.1016/j.addr.2009.10.004.
[21] H. Cabral, K. Miyata, K. Osada, K. Kataoka, Block copolymer micelles in nanomedicine applications, Chem. Rev. 118 (2018) 6844–6892, https://doi.org/10.1021/acs.chemrev.8b00199.
[22] A. Varela-Moreira, Y. Shi, M.H.A.M. Fens, T. Lammers, W.E. Hennink, R. M. Schiffelers, Clinical application of polymeric micelles for the treatment of cancer, Mater Chem Front 1 (2017) 1485–1501, https://doi.org/10.1039/c6qm00289g.
[23] P. Chytil, L. Kostka, T. Etrych, Hpma copolymer-based nanomedicines in controlled drug delivery, J Pers Med 11 (2021) 1–22, https://doi.org/10.3390/jpm11020115.
[24] T. Lammers, K. Ulbrich, HPMA copolymers: 30 years of advances, Adv. Drug Deliv. Rev. 62 (2010) 119–121, https://doi.org/10.1016/j.addr.2009.12.004.
[25] Y. Shi, R. Van Der Meel, B. Theek, E.O. Blenke, E.H.E. Pieters, M.H.A.M. Fens, J. Ehling, R.M. Schiffelers, G. Storm, C.F. Van Nostrum, T. Lammers, W.E. Hennink, Complete Regression of Xenograft Tumors upon Targeted Delivery of Paclitaxel via π-π Stacking Stabilized, ACS Nano 9 (4) (2015) 3740–3752, https://doi.org/10.1021/acsnano.5b00929.
[26] A.A. Shalmani, A. Wang, Z. Ahmed, M. Sheybanifard, R. Mihyar, E.M. Buhl, M. Pohl, W.E. Hennink, F. Kiessling, J.M. Metselaar, Y. Shi, T. Lammers, Q. Peña, Tunable polymeric micelles for taxane and corticosteroid co-delivery, Drug Deliv. Transl. Res. (2023), https://doi.org/10.1007/s13346-023-01465-x.
[27] I. Biancacci, D. De Santis, E. Rama, K. Benderski, J. Momoh, R. Pohlberger, D. Moeckel, L. Kaps, C.J.F. Rijcken, J. Prakash, M. Thewissen, F. Kiessling, Y. Shi, Q. Peña, A.M. Sofias, L. Consolino, T. Lammers, Repurposing tamoxifen for tumor microenvironment priming and enhanced tumor-targeted drug delivery, Adv Ther (Weinh) 6 (2023), https://doi.org/10.1002/adtp.202300098.
[28] Y. Shi, M.J. Van Steenbergen, E.A. Teunissen, L. Novo, S. Gradmann, M. Baldus, C. F. Van Nostrum, W.E. Hennink, Π-Π stacking increases the stability and loading capacity of thermosensitive polymeric micelles for chemotherapeutic drugs, Biomacromolecules 14 (2013) 1826–1837, https://doi.org/10.1021/bm400234c.
[29] M. Bagheri, J. Bresseleers, A. Varela-Moreira, O. Sandre, S.A. Meeuwissen, R. M. Schiffelers, J.M. Metselaar, C.F. Van Nostrum, J.C.M. Van Hest, W.E. Hennink, Effect of formulation and processing parameters on the size of mPEG- b-p(HPMA-Bz) polymeric micelles, Langmuir 34 (2018) 15495–15506, https://doi.org/10.1021/acs.langmuir.8b03576.
[30] C. Liang, X. Bai, C. Qi, Q. Sun, X. Han, T. Lan, H. Zhang, X. Zheng, R. Liang, J. Jiao, Z. Zheng, J. Fang, P. Lei, Y. Wang, D. Möckel, J.M. Metselaar, G. Storm, W. E. Hennink, F. Kiessling, H. Wei, T. Lammers, Y. Shi, B. Wei, Π electron-stabilized polymeric micelles potentiate docetaxel therapy in advanced-stage gastrointestinal cancer, Biomaterials 266 (2021), https://doi.org/10.1016/j.biomaterials.2020.120432.
[31] C.J.F. Rijcken, F. De Lorenzi, I. Biancacci, R.G.J.M. Hanssen, M. Thewissen, Q. Hu, F. Atrafi, R.M.J. Liskamp, R.H.J. Mathijssen, I.H.C. Miedema, C.W. Menke - van der Houven van Oordt, G.A.M.S. van Dongen, D.J. Vugts, M. Timmers, W.E. Hennink, T. Lammers, Design, development and clinical translation of CriPec®-based core-crosslinked polymeric micelles, Adv. Drug Deliv. Rev. 191 (2022), https://doi.org/10.1016/j.addr.2022.114613.
[32] Y. Shi, M.J. Van Steenbergen, E.A. Teunissen, L. Novo, S. Gradmann, M. Baldus, C. F. Van Nostrum, W.E. Hennink, Π-Π stacking increases the stability and loading capacity of thermosensitive polymeric micelles for chemotherapeutic drugs, Biomacromolecules 14 (2013) 1826–1837, https://doi.org/10.1021/bm400234c.
[33] M. Tiboni, M. Tiboni, A. Pierro, M. Del Papa, S. Sparaventi, M. Cespi, L. Casettari, Microfluidics for nanomedicines manufacturing: an affordable and low-cost 3D

printing approach, Int. J. Pharm. 599 (2021), https://doi.org/10.1016/j.ijpharm.2021.120464.
[34] M. Sheybanifard, N. Beztsinna, M. Bagheri, E.M. Buhl, J. Bresseleers, A. Varela-Moreira, Y. Shi, C.F. van Nostrum, G. van der Pluijm, G. Storm, W.E. Hennink, T. Lammers, J.M. Metselaar, Systematic evaluation of design features enables efficient selection of Π electron-stabilized polymeric micelles, Int. J. Pharm. 584 (2020), https://doi.org/10.1016/j.ijpharm.2020.119409.
[35] C.R. Bernau, M. Knödler, J. Emonts, R.C. Jäpel, J.F. Buyel, The use of predictive models to develop chromatography-based purification processes, Front. Bioeng. Biotechnol. 10 (2022), https://doi.org/10.3389/fbioe.2022.1009102.
[36] W. Abdelwahed, G. Degobert, S. Stainmesse, H. Fessi, Freeze-drying of nanoparticles: formulation, process and storage considerations, Adv. Drug Deliv. Rev. 58 (2006) 1688–1713, https://doi.org/10.1016/j.addr.2006.09.017.
[37] T.M. Amis, J. Renukuntla, P.K. Bolla, B.A. Clark, Selection of cryoprotectant in lyophilization of progesterone-loaded stearic acid solid lipid nanoparticles, Pharmaceutics 12 (2020) 1–15, https://doi.org/10.3390/pharmaceutics12090892.
[38] T. Ojha, Q. Hu, C. Colombo, J. Wit, M. van Geijn, M.J. van Steenbergen, M. Bagheri, H. Königs-Werner, E.M. Buhl, R. Bansal, Y. Shi, W.E. Hennink, G. Storm, C.J.F. Rijcken, T. Lammers, Lyophilization stabilizes clinical-stage core-crosslinked polymeric micelles to overcome cold chain supply challenges, Biotechnol. J. 16 (2021) e2000212, https://doi.org/10.1002/biot.202000212.
[39] C. Di Tommaso, C. Como, R. Gurny, M. Möller, Investigations on the lyophilisation of MPEG-hexPLA micelle based pharmaceutical formulations, Eur. J. Pharm. Sci. 40 (2010) 38–47, https://doi.org/10.1016/j.ejps.2010.02.006.
[40] A.O. Nornoo, D.W. Osborne, D.S.L. Chow, Cremophor-free intravenous microemulsions for paclitaxel. I: formulation, cytotoxicity and hemolysis, Int. J. Pharm. 349 (2008) 108–116, https://doi.org/10.1016/j.ijpharm.2007.07.042.
[41] J. Bresseleers, M. Bagheri, C. Lebleu, S. Lecommandoux, O. Sandre, I.A.B. Pijpers, A.F. Mason, S. Meeuwissen, C.F. van Nostrum, W.E. Hennink, J.C.M. van Hest, Tuning size and morphology of mpeg-b-p(Hpma-bz) copolymer self-assemblies using microfluidics, Polymers (Basel) 12 (2020) 1–18, https://doi.org/10.3390/polym12112572.
[42] S. Dean Allison, M.C. Molina, T.J. Anchordoquy, Stabilization of lipid/DNA complexes during the freezing step of the lyophilization process: the particle isolation hypothesis, Biochim. Biophys. Acta 1468 (2000) 127–138, https://doi.org/10.1016/s0005-2736(00)00251-0.
[43] J. Beirowski, S. Inghelbrecht, A. Arien, H. Gieseler, Freeze drying of nanosuspensions, 2: the role of the critical formulation temperature on stability of drug nanosuspensions and its practical implication on process design, J. Pharm. Sci. 100 (2011) 4471–4481, https://doi.org/10.1002/jps.22634.